MIJST
MIST International Journal of Science and Technology

Numerical Investigation for Flexural Response of Stainless-Steel Reinforced Concrete Beams

Nusrat Tabassum[1], Abdullah Al-Moneim[1,*], Said Razu[1], Aziz Ahmed[2], Khondaker Sakil Ahmed[1]

[1]Department of Civil Engineering, Military Institute of Science and Technology, Dhaka, Bangladesh
[2]School of Civil, Mining, Environmental and Architectural Engineering, University of Wollongong, Australia

***Corresponding Email:** *moneim@ce.mist.ac.bd*

ARTICLE INFO

Article History:

Received: 2th July 2025
Revised: 4th July 2025
Accepted: 06th October 2025
Published: 30th December 2025

Keywords:

Stainless steel rebar
Finite element analysis
Flexural response
Ultimate capacity

ABSTRACT

Stainless steel (SS) is becoming increasingly popular as reinforcement across the globe, owing to its superior mechanical and durability properties. This study numerically investigates the flexural behavior of concrete beams reinforced with stainless steel. Primarily, the experimental results are validated by developing 3D finite element (FE) models with stainless steel rebars, considering the actual test data. In the modelling process, 8-node brick element for concrete and 2-node beam element for reinforcement were employed in the finite element model. The numerical results are presented in terms of load displacement response, yield, and ultimate capacity with respective deformation, ductility, etc. The numerical results depicted reasonably good precision in predicting the load deformation response and ultimate load of the concrete beam reinforced with stainless-steel. The models have been regenerated for concrete beams with conventional mild steel to investigate the comparative behaviour in terms of significant changes in their load-carrying capacity and the corresponding ultimate deformation. Results revealed that the peak loads remained approximately the same for 30 MPa and 40 MPa concrete strengths, although the stainless-steel reinforced beams showed greater deformability and ductility. In addition, a parametric study of reinforced concrete beam models consisting of Grade 201 stainless steel rebars and 60-grade mild steel rebars with varying concrete grades of 30 MPa, 40 MPa, and 50 MPa was also performed to inspect their influence on the initial stiffness, ductility, and ultimate load-carrying capability of the concrete beams. The numerical response rendered that beams reinforced with stainless steel provide similar ultimate flexural capacity with improved stiffness and ductility in contrast to that of the mild steel rebars.

1. INTRODUCTION

Reinforced concrete is the outcome of the process where the limitations of concrete, such as minimal tensile strength, brittle nature, are excluded with the addition of reinforcing steel in concrete. Since the late nineteenth century, high tensile strength steel has been used to reinforce concrete, mainly in areas where concrete's minimal tensile strength would limit the member's load-carrying capacity. The reinforcing steel in reinforced concrete provides ductility and strength by bonding and anchoring to the concrete. The deterioration of steel, concrete, or both can severely diminish this bond, compromising the concrete structure's durability. The concrete must be of adequate durability to resist any chemical and physical variables that may influence the structure while also protecting the reinforcing steel embedded in it (Kapasny & Zembo, 1993). Steel deterioration is typically caused by corrosion, which is one of the key reasons of reinforced concrete's low durability (Fu & Chung, 1997). Given that steel is corrosive and less fire-resistant, engineers faced a novel challenge in obtaining a specific steel composition that met all of the requirements. One of the study's breakthroughs was the use of stainless steel (SS). SS is versatile and can be used for aesthetics and structural stability (Baddoo, 2008; Corradi, Di Schino, Borri, & Rufini, 2018; Rossi, 2014). Studies demonstrate that SS is more ductile than mild steel (MS) and reasonably more plastic in its characteristics between the yield and ultimate tensile stress, also has an outstanding toughness at low temperatures, and a degree of anisotropy (Farzana & Ahmed, 2020; Gardner, 2005; Gedge, 2008). High-strength stainless steel offers sufficient structural strength and is highly corrosion-resistant. The corrosive behaviour of three low-cost stainless steels with low nickel content demonstrated that the samples remained in a passive state even under the

maximum chloride contamination level that is naturally found in the environment (Gedge, 2008). Stainless steel demonstrated the best corrosion resistance among a range of galvanized reinforcing bars tested (Gedge, 2008). Furthermore, for any construction, ductility is a crucial problem because it is directly related to energy dissipation and structural endurance during any seismic event. Hot-rolled austenitic and duplex SS are about three times more ductile compared to conventional carbon steel (Saraswathy & Song, 2005). However, stainless steel is a difficult material to work with owing to its diverse alloy composition. This research conducts a comparative investigation of MS and SS reinforced concrete.

Extensive experiments to determine the bond behavior of steel and concrete, stress generation at each point, and various properties such as ductility and corrosion resistance capacity, under different loading patterns are tedious, time-consuming, and expensive due to the complex setup. To address all of these restrictions, numerical modeling was performed. The task of designing and analyzing any structural member with variable material properties, boundary conditions, and loading patterns became very simple with the aid of numerical modelling, which required no significant setup. In a numerical study, a cross-section layer model and the stiffness matrix method are used to simulate the deflection of beams that failed in bending at any load level. To accurately predict the force-midspan deformation relationship in the tested beams, this numerical strategy utilized the material properties obtained from experimental tests. This showed that the approach is adequate for simulating the behaviour of RC beams reinforced by the near surface mounted (NSM) strengthening procedure using carbon fibre reinforced polymer (CFRP) laminate strips (Barros & Fortes, 2005). The dynamic response of RC beams under varying rates of point loading was studied using LS-DYNA, an explicit finite element program. The test program yielded a significant amount of test data, including load vs. mid-span deformation, crack profiles, strain at the mid-point of longitudinal tensile reinforcement acceleration at many sites along the specimens (Adhikary, Li, & Fujikake, 2012).

This paper examined mild steel and concrete beams reinforced with stainless steel using finite element analysis. Primarily, the numerical models of both MS and SS reinforced concrete beams have been validated with existing experimental data (Ahmed, Habib, & Asef, 2021; Saatci & Vecchio, 2009). Results are extracted in terms of load deformation response, stress distribution, and failure pattern. In addition, a parametric analysis was carried out to determine the impact of various concrete grades on both MS and SS.

2. METHODOLOGY

In experimental testing of beams, stress transfer occurs at the steel-concrete interface after the load application. Fine fractures form as a result of an imbalanced stress distribution. These cracks develop over time and eventually cause the structural member to disintegrate. Finite element models were developed to facilitate the determination of failure loads and displacements, stress generation, load deflection curves, and failure patterns. Two-step validation was done using numerical models for separate experimental test beams. Firstly, an experimental simply supported RC beam with no shear reinforcement was validated (Saatci & Vecchio, 2009). Later, from another study, both SS reinforced beams and MS reinforced beams were validated (Ahmed et al., 2021). Lastly, using the numerical models for both SS and MS reinforced beams, a parametric study for varying concrete strength was carried out.

2.1 SPECIMEN DETAILS

2.1.1 FE MODEL FOR VALIDATION OF EXPERIMENTAL TEST RESULTS

This section's static analysis replicates the experiments on RC beams conducted by Saatci (2007) (Saatci & Vecchio, 2009). The outcomes of the study were compared against the experimental test results after the static beam was modelled in ABAQUS (2012) using the FE technique. To gain a better understanding of how shear reinforcement affects failure behaviour, the experimental test was carried out on four simply supported RC beams. These beams were supplied with same longitudinal reinforcement and varying shear reinforcement. This study's validation used the beam specimen MS0, which had no shear reinforcement. The RC beam tested in the previous analysis is shown in **Figure 1**.

2.1.2 EXPERIMENTAL TEST OF STAINLESS AND MILD STEEL REBAR REINFORCED BEAMS

The current investigation modelled a mild steel reinforced and another SS reinforced concrete beam with a cross-sectional area of 150 mm x 200 mm and a length of 1500 mm (Ahmed et al., 2021). A loading plate of cross-sectional area 150 mm x 50 mm and length of 500 mm was also modelled, and the displacement was placed on top of it. Two cylinders with a diameter of 100 mm and a length of 150 mm were positioned beneath the beam, with two more cylinders of identical geometry inserted between the RC beam and the loading plate. The load vs. displacement graphs were acquired for the beams' mid-span section.

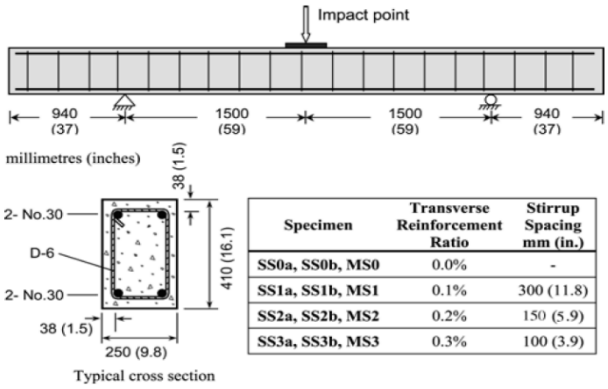

Specimen	Transverse Reinforcement Ratio	Stirrup Spacing mm (in.)
SS0a, SS0b, MS0	0.0%	-
SS1a, SS1b, MS1	0.1%	300 (11.8)
SS2a, SS2b, MS2	0.2%	150 (5.9)
SS3a, SS3b, MS3	0.3%	100 (3.9)

Figure 1: Experimental test setup (Saatci & Vecchio, 2009)

2.2 MATERIAL MODELLING

The beam model's concrete compressive strength was around 50 MPa during validation testing, and mild steel rebars of Grade 60 were used. Later, beams reinforced with stainless steel and mild steel were modelled and validated using previously conducted experimental tests. A comparative investigation of beams reinforced with stainless steel and mild steel was conducted. Furthermore, a parametric investigation of these beams reinforced with stainless and mild steel for varied concrete strengths was carried out. **Figure 2** provides information on the material properties of SS adopted in this study.

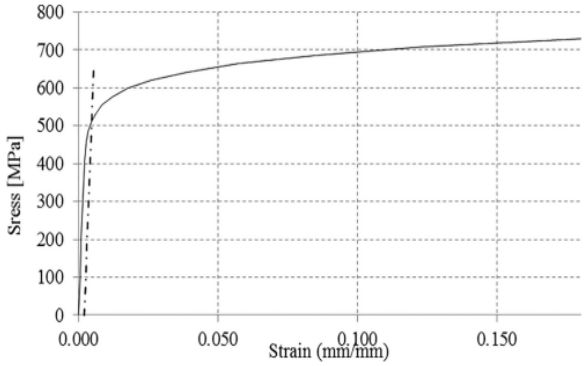

Figure 2: Typical mechanical properties of the 201 grade plain SS rebar

The elastic properties of concrete of varying compressive strength are presented in Table 1.

Table 1: Elastic property of varying concrete strength (Hafezolghorani, Hejazi, Vaghei, Jaafar, & Karimzade, 2017)

Concrete Strength (MPa)	Young's Modulus (MPa)	Poisson's Ratio
30	25918.92	0.2
40	30000	0.2
50	32795.2	0.182

Similarly, the plastic properties of varying concrete grades are provided in Table 2.

Table 2: Plastic properties of concrete of varying concrete strength (Hafezolghorani et al., 2017)

Concrete Strength (MPa)	Dilation Angle	Eccentricity	fb0/fc0	K	Viscosity Parameter
30	31	0.1	1.16	0.67	0
40	31	0.1	1.16	0.67	0
50	38	0.1	1.16	0.66	0

Finally, the tensile properties of various concrete grades adopted in the study are presented in Table 3.

Table 3: Tensile behaviour of concrete of varying concrete strength (Hafezolghorani et al., 2017)

Concrete Strength (MPa)	Yield Stress (MPa)	Inelastic Strain
30	3	0
	0.03	0.001167315
40	4	0
	0.04	0.001333333
50	5	0
	0.05	0.001494322

Additionally, the material properties of 60-grade mild steel are presented in Table 4.

Table 4: Mild (MS) and stainless steel (SS) properties

Type	Density (tonne / mm^3)	Elasticity		Plasticity	
		Young's Modulus (MPa)	Poisson's Ratio	Yield Stress (MPa)	Plastic Strain (mm/mm)
MS	7.85E-9	200000	0.3	420	0
				532	0.00271
				551	0.0224
				655	0.114
				447	0.218
SS	7.8E-9	190000	0.28	420	0
				450	0.051
				500	0.152
				550	0.352

2.3 NUMERICAL MODELLING

The bending and shear reinforcements were coupled to the surrounding concrete utilizing the embedded model technique at each place where the concrete and reinforcing sections cross. The employment of embedded components implied the perfect bond between the reinforcement and the concrete. The CDP model aids in visualizing the pattern of damage of concrete sections as tension and compression damage. The reinforcements were simulated using simple elastic-plastic materials based on existing research. The beam was simulated at full scale to ensure the actual test behaviour, as illustrated in **Figure 3**. **Table 5** presents detailed data for numerical modelling.

Table 5: Numerical modelling details overview

Material Modelling	•	Concrete: Concrete Damage Plasticity
	•	Steel: Elasto Plastic Steel
Element	•	Concrete: C3D8R

Type	• Steel: B31
Element Interface	• Embedded Model
Contact Algorithms	• Mechanical Constraint Formulation: Penalty Contact Method • Contact Property: Coulomb Friction • Method: Tangential Behavior - Friction Coefficient (0.25) • Normal Behavior: Pressure over-closure- "Hard" contact.
Mesh Size	• 25 mm for validation test beam by Saatci (2007). • 20 mm for comparative and parametric study test beam reinforced with stainless steel and mild steel rebars.
Loading Protocol	• Displacement control. • A supporting steel plate with 1-inch thickness was used for the validation test beam by Saatci (2007). • For the beams modelled for comparative and parametric study, a downward displacement of 30mm was applied to the upper surface of the plate placed over the cylinders.
Boundary Conditions	• The lower outer surfaces of two of the beams are made encastred. • The plate and cylinders' x-directional and z-directional movements are restrained.

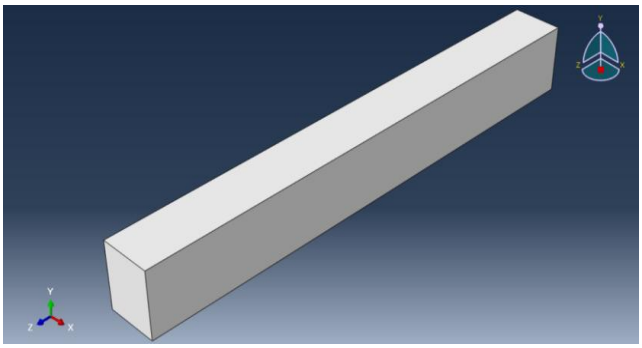

(a)

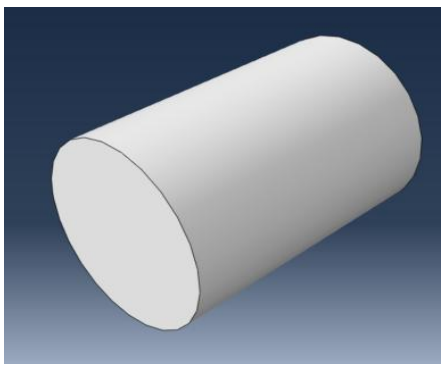

(b)

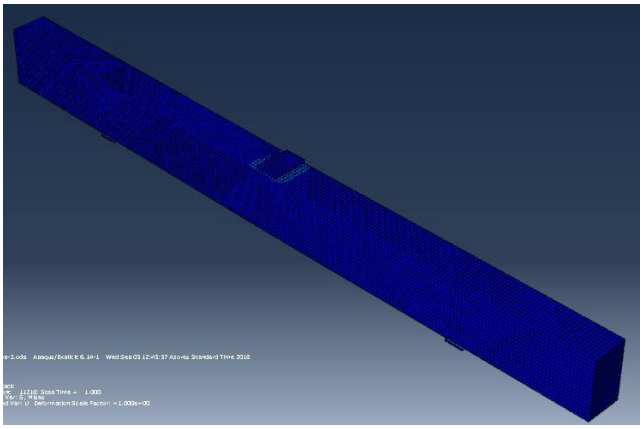

(c)

Figure 3: (a)-(b) Model development using parts in Abaqus CAE, (c) Meshing of the developed model.

3. RESULTS AND DISCUSSIONS

3.1 NUMERICAL VALIDATION OF TEST BEAM BY SAATCI (2007)

The schematic view of the numerical model of the test beam (Saatci & Vecchio, 2009) is illustrated in Fig. 3(c). The load deformation curve of the beam MS0 is presented in **Figure 4**. The load was applied to the beam at midspan by a bearing plate, and the analysis was performed using the explicit approach of ABAQUS (2012). As a result, the stiffness, or static load, of the beam has been calculated using the reaction force between the beam's contact surface and the loading plate. Data fluctuation was detected during testing because of non-linear complex deformation when the load increased, and crack propagation occurred.

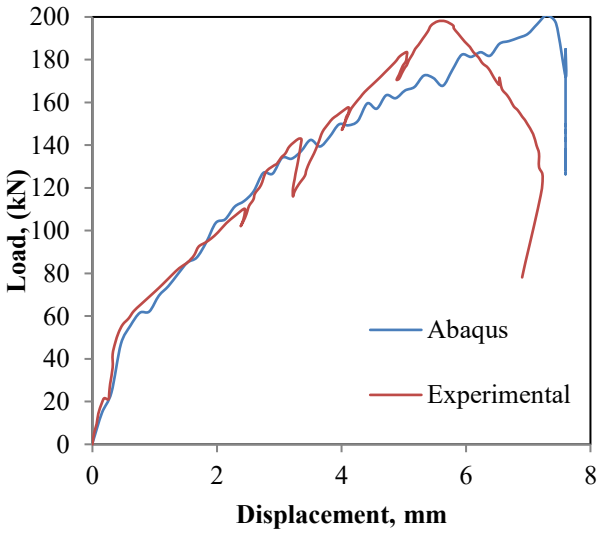

Figure 4: Comparison of load deformation response between numerically analysed beam (MS0) with experimental test result obtained by (Saatci & Vecchio, 2009)

This phenomenon is also noticed during flexural tests on RC beams. MS0's response via FE analysis was determined to be relatively comparable to the actual response obtained in the experiment. The beam was estimated by ABAQUS

(2012) to be somewhat more flexible than the response that was seen in the experiment. Once the peak load was reached, the main behavioral discrepancy between the expected and observed results became apparent. Using ABAQUS (2012), it was found that the beam could withstand loads up to 197.86 kN before losing its capacity at a maximum load of 200.7 kN. This implies that the numerical model was successfully developed and accurately simulated real circumstances, with a peak load prediction accuracy of 98.58%.

3.2 NUMERICAL VALIDATION FOR SS REINFORCED CONCRETE BEAM

SS reinforced concrete beams have been previously tested experimentally by Ahmed et al. (Ahmed et al., 2021). **Figure 5** depicts the deflected shape of the tested beam with stress distribution.

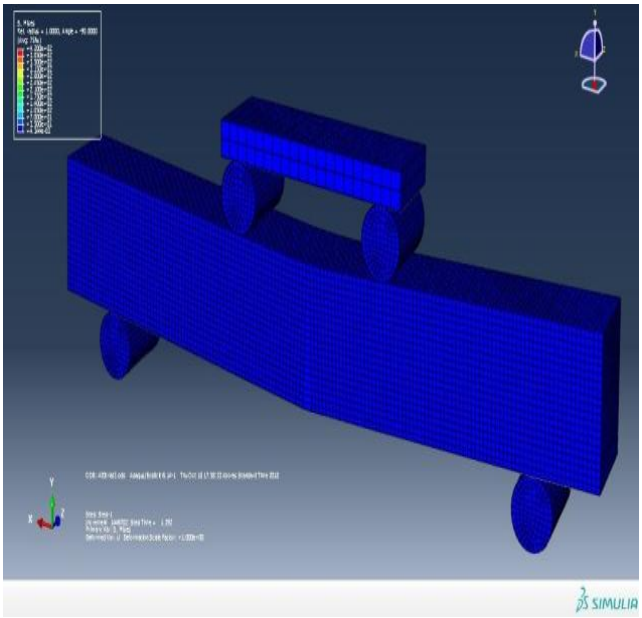

Figure 5: FE model of the tested RC beam (Ahmed et al., 2021)

For validation, a comparative analysis between experimental and numerical data for both SS reinforced concrete beams and MS reinforced concrete beams was done. In **Figure 6**, the load deformation responses of both experimental results and numerical outcomes are presented. The results indicate that the beams' ultimate flexural capacity is in good accord. The ultimate flexural capacity of the beam derived from the computational model was 72.85 kN, while the maximum load obtained for the experimental beam was 72.5 kN. The experimental curve demonstrates that the peak load is attained with a higher displacement than the numerical model curve. The experimental beam's increased displacement is owing to the incorporation of a softer material between the beam and the support. In addition, there is an initial set between the beam and support that creates a larger displacement on its own, resulting in more displacement than the ABAQUS numerical model curve.

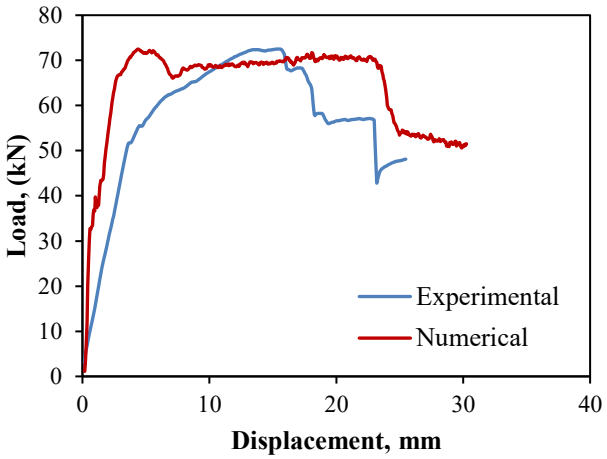

Figure 6: Load displacement response of the experimental (B50) (Saatci & Vecchio, 2009) and the numerical model of the mild steel reinforced concrete beam (MSL-2)

In the experimental and numerical curves, as shown in **Figure 7**, the peak loads are predicted satisfactorily, but the displacement of the experimental beam is more than the numerical model. The maximum load obtained for the numerical beam modelled was 71.93 kN with a corresponding displacement of 3mm, and the maximum load obtained for the experimental beam was 72.42 kN with a corresponding displacement of 18.77 mm. This phenomenon is due to the fact that the bars used in the experiment are plain stainless steel. When a load was applied, there was a slip in the contact surface, resulting in more displacement than the deformed bars. In the numerical model, the bars are embedded into the concrete surface and function as an integral part. The slip characteristics were not incorporated into the model; hence, the load vs. displacement curves vary.

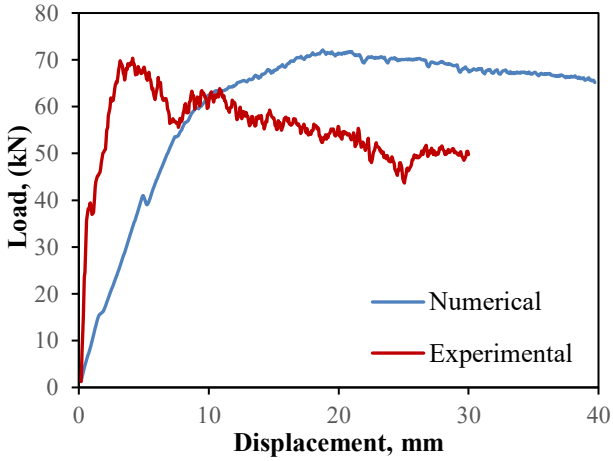

Figure 7: The load-deformation response of experimental (B50) and numerical model of stainless steel reinforced concrete beam (SSL-1)

3.3 PARAMETRIC STUDY FOR VARYING CONCRETE STRENGTHS

Figure 8 compares numerical model beams with varied concrete grades (30 MPa, 40 MPa, and 50 MPa) reinforced

with stainless steel. **Table 6** demonstrates that the SS reinforced RC beam with concrete strength 40MPa has the highest load carrying capability of 74.89 kN with a displacement of 3.65 mm. This occurs because stainless steel reinforced beams with higher-grade concrete break early due to the high ductility of SS reinforcement and lower cracking strains of higher-grade concrete, which happen before the ultimate strength of SS.

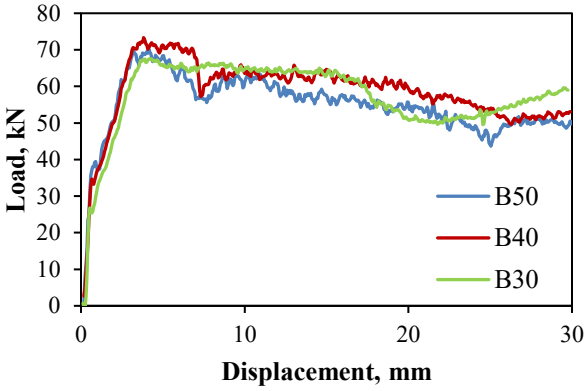

(a)

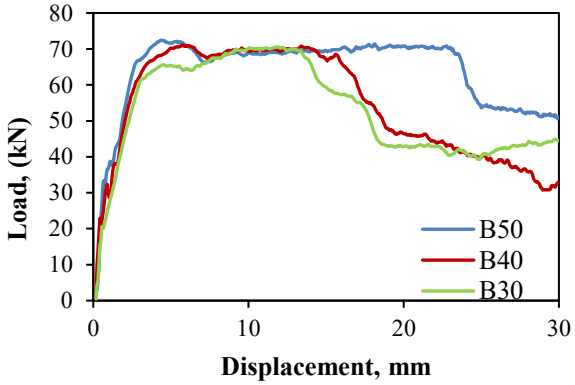

(b)

Figure 8: The load-deformation response of concrete beams reinforced with (a) stainless rebar, (b) mild steel rebar

Table 6: Peak loads for SS reinforced RC beams with varying concrete strength

Concrete Strength (MPa)	Peak Load (kN)
30	68.82
40	74.89
50	72.61

In **Figure 9**, numerical model beams with varying concrete grades (30 MPa, 40 MPa, and 50 MPa) reinforced with stainless steel are compared. From **Table 7**, it is observed that the MS reinforced RC beam with concrete strength 50 MPa has the highest load carrying capacity of 72.85 kN with corresponding displacement 4.33 mm.

Table 7: Peak loads for MS reinforced RC beams with varying concrete strength

Concrete Strength (MPa)	Peak Load (kN)
30	65.7
40	71.37
50	72.85

3.4 COMPARATIVE STUDY BETWEEN STAINLESS STEEL REINFORCED BEAM AND MILD STEEL REINFORCED BEAM

The load deformation response of MS and SS reinforced beams developed with three different concrete grades is generated as part of the parametric analysis using the numerical models shown in **Figure 9** (a), (b), and (c). The statistics show that stainless steel has equivalent or larger peak loads than mild steel. At 30 MPa concrete strength, MS has a greater peak load than SS. This is owing to the fact that the findings are dependent on concrete modelling and confinement. When the beam was modelled, the connection between concrete and stainless steel was not adequately characterized. This resulted in a minor divergence. This could possibly be related to the fact that stainless steel reinforced beams break earlier due to high ductility cracking strain, which occurs before the ultimate strength of SS.

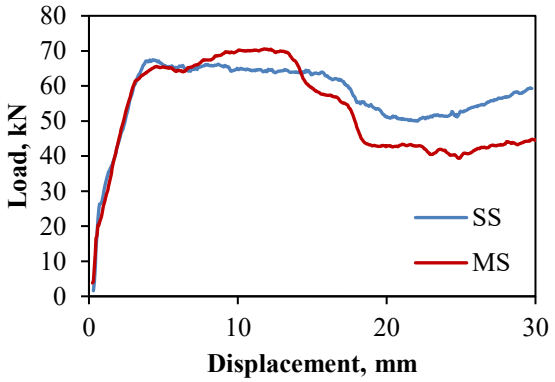

(a)

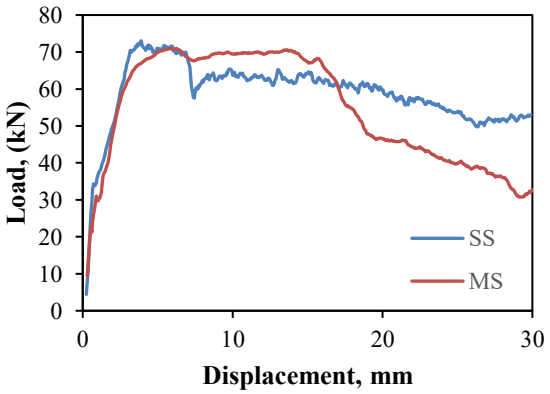

(b)

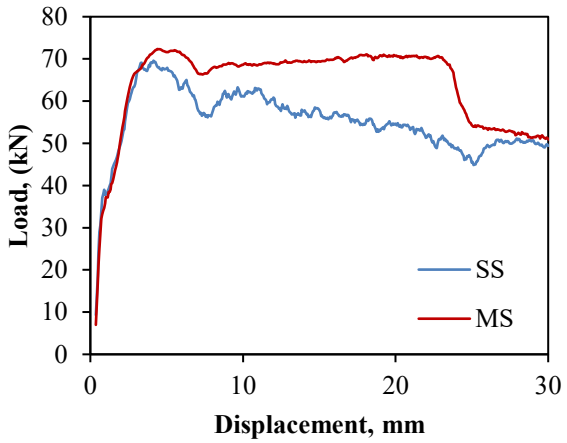

(c)

Figure 9: Comparison of Load - Load-displacement responses SS and MS reinforced concrete beams with (a) 30, (b) 40, and (c) 50 MPa Concrete Strength.

In **Table 8**, the peak loads for MS reinforced concrete beams and SS reinforced concrete beams with varying concrete grades are tabulated. From this table, it is observed that SS reinforced beams show a greater load-carrying capacity than mild steel reinforced beams.

Table 8: Peak Loads for MS reinforced concrete beam vs. SS reinforced concrete beam with varying concrete grade

Concrete Strength (MPa)	Peak Load (SS bar) (kN)	Peak Load (MS bar) (kN)
30	68.58	70.95
40	74.89	71.37
50	72.61	72.85

4. CONCLUSIONS

In this study, the finite element technique was used to analyze the flexural response of concrete beams reinforced stainless steel. Numerical models were evaluated against experimental data for both MS and SS. The influence of the concrete grade on the flexural response was also observed using numerical simulations. Based on the analyses, the following conclusions can be derived:

1. The numerical model for mild steel reinforced concrete beams demonstrated good agreement with the test results claimed by Saatci (2007), with an accuracy of 98.58% in predicting ultimate flexural capacity. In the instance of a mild steel reinforced concrete beam, the peak value of the numerical analysis is 0.48% higher than the experimental result. In contrast, the initial stiffness of numerical analysis is greater. This is because geometric nonlinearities were not incorporated, as well as certain test setup shortcomings.
2. In the case of stainless steel reinforced concrete beams, the numerical models also predicted the ultimate load quite precisely with an accuracy of 99.32%. However, the initial stiffness of the experimental analysis was found to be lower due to test setup shortcomings.
3. In the instance of SS reinforced concrete beams with variable concrete strength, peak values, stiffness, and ductility were accurately predicted and proved to be almost identical for all B30, B40, and B50 concrete strengths. This is because flexural failure occurs at the reinforcing ends; therefore, increasing concrete strength does not improve the flexural capacity of beams.
4. In comparison with the SS reinforced concrete beam and the MS reinforced concrete beam with 30 and 40 MPa concrete, the ductility of the SS reinforced concrete beam was found to be higher than the conventional MS rebar.
5. The validated model prepared in this study can provide the basis for subsequent experimental and numerical studies planned by the authors on the properties of concrete reinforced with stainless steel rebars.

ACKNOWLEDGMENTS

The authors gratefully recognize the support provided by the Concrete lab and the Structural Mechanics lab of the Civil Engineering department of MIST during the preparation and testing of the experimentally investigated beams.

DATA AVAILABILITY STATEMENT

Datasets generated during the current study are available from the corresponding author upon reasonable request.

FUNDING DECLARATION

This research was self-funded.

ETHICS APPROVAL

This study is an engineering experimental investigation. The MIJST Research Ethics Committee has confirmed that formal ethical approval was not required.

ETHICS, CONSENT TO PARTICIPATE, AND CONSENT TO PUBLISH

Not applicable.

COMPETING INTERESTS

The authors declare that they have no competing interests.

AUTHOR CONTRIBUTIONS

Author 1: Nusrat Tabassum - Writing: Original draft, Formal analysis, Software, Validation

Author 2: Abdullah Al Moneim - Writing: Review and editing, Visualization

Author 3: Aziz Ahmed - Writing: Review and editing

Author 4: Khondaker Sakil Ahmed - Writing: Review and editing, Supervision

ARTIFICIAL INTELLIGENCE ASSISTANCE STATEMENT

Portions of this manuscript were assisted by an artificial intelligence language model (ChatGPT, OpenAI). The tool was used solely for language editing, text refinement, and clarity improvement. All content, data interpretation, analysis, conclusions, and final decisions were generated, verified, and approved by the authors. The authors take full responsibility for the accuracy and integrity of the manuscript.

CONFLICT OF INTEREST DECLARATION

The authors declare that they have no conflicts of interest.

REFERENCES

Adhikary, S. D., Li, B., & Fujikake, K. (2012). Dynamic behavior of reinforced concrete beams under varying rates of concentrated loading. *International Journal of Impact Engineering, 47*, 24-38.

Ahmed, K. S., Habib, M. A., & Asef, M. F. (2021). *Flexural response of stainless steel reinforced concrete beam.* Paper presented at the Structures.

Baddoo, N. (2008). Stainless steel in construction: A review of research, applications, challenges and opportunities. *Journal of constructional steel research, 64*(11), 1199-1206.

Barros, J. A., & Fortes, A. (2005). Flexural strengthening of concrete beams with CFRP laminates bonded into slits. *Cement and Concrete Composites, 27*(4), 471-480.

Corradi, M., Di Schino, A., Borri, A., & Rufini, R. (2018). A review of the use of stainless steel for masonry repair and reinforcement. *Construction and Building Materials, 181*, 335-346.

Farzana, K., & Ahmed, K. (2020). *Performance based seismic analysis of stainless steel reinforced concrete bridge pier using damping ductility relationship.* Paper presented at the IABSE-JSCE Joint Conference on Advances in Bridge Engineering-IV August.

Fu, X., & Chung, D. (1997). Effect of corrosion on the bond between concrete and steel rebar. *Cement and Concrete Research, 27*(12), 1811-1815.

Gardner, L. (2005). The use of stainless steel in structures. *Progress in Structural Engineering and Materials, 7*(2), 45-55.

Gedge, G. (2008). Structural uses of stainless steel—buildings and civil engineering. *Journal of constructional steel research, 64*(11), 1194-1198.

Hafezolghorani, M., Hejazi, F., Vaghei, R., Jaafar, M. S. B., & Karimzade, K. (2017). Simplified damage plasticity model for concrete. *Structural engineering international, 27*(1), 68-78.

Kapasny, L., & Zembo, S. (1993). *The influence of the reinforcement corrosion on the load-bearing capacity of the reinforced concrete structures.* Paper presented at the Proc. Int. Conf. RILEM. Bratislava.

Rossi, B. (2014). Discussion on the use of stainless steel in constructions in view of sustainability. *Thin-Walled Structures, 83*, 182-189.

Saatci, S., & Vecchio, F. J. (2009). Effects of shear mechanisms on impact behavior of reinforced concrete beams. *ACI structural Journal, 106*(1), 78.

Saraswathy, V., & Song, H. W. (2005). Performance of galvanized and stainless steel rebars in concrete under macrocell corrosion conditions. *Materials and Corrosion, 56*(10), 685-691.